The nonequilibrium solutions of Leibowitz and Kuo yield small values of $n_H(2)$ behind the shock compared to the Boltzmann distribution (equilibrium) value, because they considered not only thermal nonequilibrium and finite ionization, but also finite excitation. According to Eq. (2) low values of $n_H(2)$ decrease the radiative flux relative to equilibrium. Thus, Leibowitz and Kuo predicted that nonequilibrium reduces the radiative flux.

Table 1 gives values of $n_H(2)$ for the assumption that it is Boltzmann populated at T_e or that it is populated in equilibrium with n_e. The necessary data for T_e, n_H, and n_e were obtained from the solution of Tiwari and Szema shown in Figs. 1 and 2. Note that for the Boltzmann distribution, $n_H(2)$ is much greater than it is for the assumption that $n_H(2)$ and n_e exist in equilibrium at T_e. The assumptions used to calculate $n_H(2)$ are the major reasons for the opposite conclusions of Tiwari and Szema and Leibowitz and Kuo.

The discussion to this point has been limited to the optically thin approximation and the Balmer region of the spectrum; however, the conclusions are generally valid. Figure 3 shows that the ground state continuum radiation is optically thick; thus, only the gas near the body contributes to radiative heating of the body in that spectral region. The atomic line transitions are also optically thick near the line center, so the line centers contribute to radiative heating only if the radiation is emitted close to the body. The free-free continuum transitions occur mainly in the spectral range below 2 eV. The free-free continuum radiation can be important; however, at the temperatures of interest its contribution to the flux is small, because of its small source function. Consequently, the radiative heating comes mainly from the Balmer region of the spectrum, where the shock layer is optically thin, and the above approximations hold.

Acknowledgment

This research was supported by NASA Langley Research Center, Hampton, Va., under Contract NASA NAG 1-125.

References

[1]Leibowitz, L.P., "Measurements of the Structure of an Ionizing Shock Wave in a Hydrogen-Helium Mixture," *Physics of Fluids*, Vol. 16, 1973, p. 59.

[2]Leibowitz, L.P. and Kuo, Ta-Jin, "Ionizational Nonequilibrium Heating During Outer Planetary Entries," *AIAA Journal*, Vol. 14, Sept. 1976, p. 1324.

[3]Tiwari, S.N. and Szema, K.Y., "Effects of Precursor Heating on Chemical and Radiative Nonequilibrium Viscous Flow Around a Jovian Entry Body," *Progress in Astronautics and Aeronautics: Outer Planet Entry Heating and Thermal Protection*, Vol. 64, edited by R. Viskanta, AIAA, New York, 1979, pp. 129-146.

[4]Tiwari, S.N. and Szema, K.Y., "Effects of Precursor Heating on Radiating and Chemically Reacting Viscous Flow Around a Jovian Entry Body," NASA CR-3186, Sept. 1979.

[5]Zoby, E.V. and Moss, J.M., "Preliminary Thermal Analysis for Saturn Entry," *Progress in Astronautics and Aeronautics: Aerothermodynamics and Planetary Entry*, Vol. 77, edited by A.L. Crosbie, AIAA, New York, 1981, pp. 374-395.

[6]Moss, J.M., "A Study of the Aerothermal Entry Environment for the Galileo Probe," *Progress in Astronautics and Aeronautics: Entry Heating and Thermal Protection*, Vol. 69, edited by W.B. Olstad, AIAA, New York, 1980, pp. 3-25.

[7]Nelson, H.F., "Effect of a Finite Ionization Rate on the Radiative Heating of Outer Planet Atmospheric Entry Probes," NASA CR-3577, June 1982.

[8]Zel'dovich, Ya. B. and Raizer, Yu. P., *Physics of Shock Waves and High-Temperature Hydrodynamic Phenomena*, Academic Press, New York, 1966.

[9]Zoby, E.V., Sutton, K., Olstad, W.B. and Moss, J.M., "An Approximate Inviscid Radiating Flow-Field Analysis for Outer Planet Entry Probes," *Progress in Astronautics and Aeronautics: Outer Planet Entry Heating and Thermal Protection*, Vol. 64, edited by R. Viskanta, AIAA, New York, 1979, pp. 42-64.

Effect of Low Reynolds Number Turbulence Amplification on the Galileo Probe Flowfield

R. N. Gupta* and J. N. Moss†
NASA Langley Research Center, Hampton, Virginia

Introduction

IN a recent paper, Moss and Simmonds[1] presented the forebody flowfield solutions for Jupiter entry conditions for a 335-kg probe. These results for the massive ablation conditions were obtained by using the two-layer algebraic eddy-viscosity model due to Cebeci.[2,3] In this model of turbulence, the inner law is based upon Prandtl's mixing-length concept and the outer law employs the Clauser-Klebanoff expression. A value of 0.4 for the von Kármán constant k_1 appearing in the inner law and a value of 0.0168 for the constant k_2 appearing in the outer Clauser-Klebanoff expression have been employed by Moss and Simmonds[1] as suggested by the earlier work of Ref. 3. It was obtained in Ref. 4 that the variations in the inner law expression (including in the value of k_1) do not affect the value of eddy viscosity for a massively blown shock layer substantially. For such flows, the outer eddy-viscosity expression seems to play a predominant role. In the study of Ref. 4, the Cebeci model of Ref. 3 with a constant value of $k_2 = 0.0168$ was employed as the baseline model. Recent experimental studies[5] for the unblown blunt-body viscous-shock-layer flows, however, suggest that a much higher value than 0.0168 might be needed to obtain an agreement between the predictions and experimentally measured eddy-viscosity values, as shown in Fig. 1. This appears to be the result of low Reynolds number effect, which contributes to the amplification of turbulence. According to Ref. 6, a value of s/δ‡ of about 30 to 50 is required to "wash out" the low Reynolds number effect. For the Galileo probe, where the flow is assumed to undergo transition instantaneously immediately downstream of the stagnation point owing to massive ablation, a typical value of s/δ is about 15 at the end of the forebody flowfield. Therefore the low Reynolds number effect is likely to persist for the entire length of the probe and may contribute to the amplification of turbulence more for a blown surface than for an unblown surface. The purpose of this study is to evaluate the impact of this effect on the Galileo probe surface-heating and mass-loss rates, which are critical to the probe's success.

Analysis

The extent of the low Reynolds number amplification is indicated in the figure inset in Fig. 2 (taken from Ref. 7) where the mixing length, $(l/\delta)_{max}$, was derived from the experimental velocity profiles for flat plates, cones, and cylinders. Also shown in the inset figure is an extrapolation to the curve of Ref. 7 for a value of δ^+ near 100. Here δ^+ is a measure of the Reynolds number based on boundary-layer thickness δ, friction velocity $U_\tau (=\sqrt{\tau_w/\rho_w})$, and wall conditions. Although the mixing-length amplification contained in Fig. 2 (obtained for the "wall" turbulent shear flows) is not strictly applicable for "free" turbulent shear

Received Nov. 3, 1982; revision received Jan. 7, 1983.

*NRC-Senior Research Associate, Aerothermodynamics Branch, Space Systems Division. Member AIAA.

†Research Leader, Aerothermodynamics Branch, Space Systems Division. Member AIAA.

‡Various symbols used in this paper have meanings similar to those of Refs. 1 and 3.

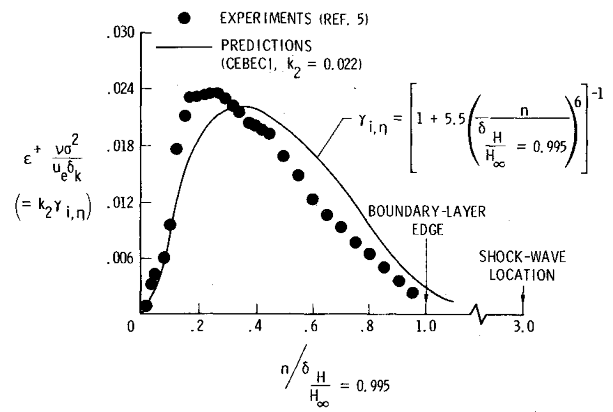

Fig. 1 Eddy-viscosity distribution for an unblown surface at $s/s_{max} = 0.951$ for $Re_{\infty,smax} = 12.4 \times 10^6$; symbols are defined in Ref. 3.

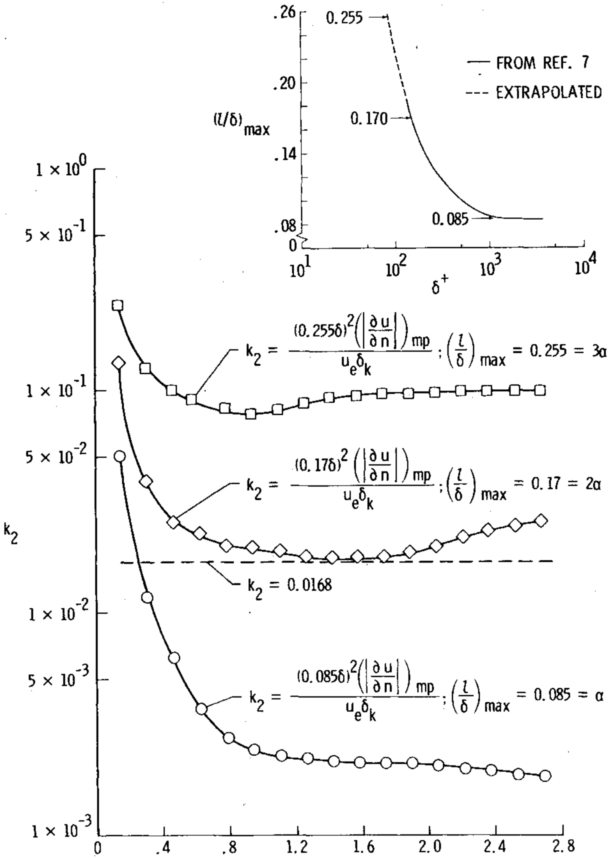

Fig. 2 Variation of k_2 (in the outer eddy-viscosity approximation) with different values of $(l/\delta)_{max}$. Inset figure gives variation of $(l/\delta)_{max}$ with δ^+ for flows over plates, cones, and cylinders.

layers (encountered with massive surface ablation), this figure still serves to provide the quantitative information, since no similar experimental results exist about the amplification of turbulence in massively blown shock layers or free shear layers. Some indication of this amplification is available in the attachment peak-heating correlation for shear layers given in Ref. 8. For a massively blown shock layer, with U_τ almost negligible, δ^+ may be of the order of 100.§ For these values of δ^+, increases of a factor of 2 or more in the mixing length, $(l/\delta)_{max}$, above the usual level of 0.085 or so are observed,[7] as shown in the inset figure of Fig. 2. In the present study, the effect of low Reynolds number amplification on Galileo probe mass-loss rate was obtained by evaluating the outer law "constant" in the Cebeci turbulence model from

$$k_2 = l^2 \left| \frac{\partial u}{\partial n} \right|_{mp} \Big/ U_e \delta_k \qquad (l/\delta)_{max} = \alpha \qquad (1)$$

where the subscript mp denotes matchpoint between the inner and outer law and α is a constant having a value of 0.085 in the absence of any low Reynolds number amplification. It may be mentioned here that Eq. (1) has been obtained by equating the outer region eddy-viscosity expressions[7] based on mixing-length approximation and the Clauser-Klebanoff formulation. Thus, knowing the amplification $(l/\delta)_{max}$ for the Reynolds number δ^+ from the inset figure in Fig. 2, the appropriate value of k_2 may be obtained iteratively from Eq. (1). For application to the present massively blown case, however, results were obtained (see Fig. 2) for three values of the mixing length, $(l/\delta)_{max}$, to quantify the role played by the low Reynolds number effect. The values chosen were one, two, and three times the nonamplified value of 0.085 to bracket its influence on mass-loss rate in the neighborhood of $\delta^+ = 100$.

In the present analysis the calculations for the surface-heating and mass-loss rates have been carried out for the 335-kg probe at 49.13 s of entry time corresponding to the peak heating conditions.[1] In these calculations (contained in Table 1) the turbulent Prandtl and Lewis numbers are assumed to be 0.9 and 1.0, respectively. Using a value of unity for the turbulent Lewis number, however, implies that the contribution from turbulent diffusion due to the species concentration gradients in the energy equation is not significant. The computations were, therefore, also made for values of $Le_T = 1.0 \pm 20\%$, since not much information is available about it. The results are provided in Table 2.

Discussion of Results

Figure 2 shows the values of outer law constant k_2 in the Cebeci model of turbulence obtained iteratively along the body stations from Eq. (1) for three values of the amplification factor α. Also shown in the same figure is the standard $k_2 = 0.0168$ value. It is clear that increases of a factor of 2 to 3 in $(l/\delta)_{max}$ near $\delta^+ = 100$ give values for k_2 at various body stations much larger than 0.0168. Even for an unamplified case ($\alpha = 0.085$) with $\delta^+ > 2000$, k_2 is not a constant at various stations along the body.

Corresponding to the four cases of Fig. 2, Table 1 gives the results for surface-heating and mass-loss rates. This table clearly shows that substantial increases in mass-loss rates are possible for δ^+ around 100. For a massively blown surface, with U_τ approaching a very small value, δ^+ would have a value of less than 100. Using a value of Le_T different from unity seems to affect the mass-loss rate to a much lesser extent, as shown in Table 2. Generally, a higher mass-loss rate is obtained by using $Le_T = 1.2$ than $Le_T = 0.8$ when compared with the values obtained by employing $Le_T = 1.0$.

From the analysis carried out here, it may be seen that increases in the mass-loss ratio from 4% to 50% are possible with the low Reynolds number amplification effect, whereas using a value of 1.2 for the turbulent Lewis number can increase the mass-loss rate from 4% to 10%. Lower values of the turbulent Lewis number and low Reynolds number amplification effect result in reducing the mass-loss rate. Even though the analysis presented depends heavily on the experimental information available for unblown shock layers for the mixing-length amplification, the present analysis does bring out the importance of such an amplification for massively ablating shock layers. A conservative accounting of

§With massive blowing, δ^+, in fact, tends toward a value much smaller than 100. However, substantial extrapolation of the curve of Ref. 7 beyond the range of the experimental data may not be very appropriate.

Table 1 Effect of low Reynolds number turbulence amplification on surface-heating and mass-loss rates for the 335-kg probe at a time of 49.13 s

Condition	$-\int_0^s \bar{q}_w^c \mathrm{d}\bar{A}$, MW		$\int_0^s \bar{q}_w^{R-} \mathrm{d}\bar{A}$, MW		$\int_0^s (\bar{\rho}\bar{v})_w \mathrm{d}\bar{A}$, kg/s		Mass-loss ratio	
(i) Standard model as of May 1982 with coupled spallation; employs standard two-layer eddy-viscosity model of Cebeci with $k_2 = 0.0168$ (without low Reynolds number turbulence amplification)	9.00[a]	15.00[b]	115.00[a]	212.00[b]	4.00[a]	7.70[b]	1.00[a]	1.00[b]
(ii) With low Reynolds number turbulence amplification: $k_2 = \ell^2 \left(\left\| \frac{\partial u}{\partial n} \right\| \right)_{mp} / U_e \delta_k$; $(\ell/\delta)_{max} = 0.085$; $\delta^+ \geq 2000$	9.00[a]	16.50[b]	88.10[a]	148.50[b]	3.00[a]	5.13[b]	0.75[a]	0.067[b]
(iii) Same as (ii) except $(\ell/\delta)_{max} = 0.17$; $\delta^+ = 105$	8.50[a]	14.61[b]	119.20[a]	222.26[b]	4.31[a]	8.00[b]	1.08[a]	1.04[b]
(iv) Same as (ii) except $(\ell/\delta)_{max} = 0.255$; $\delta^+ = 85$	6.65[a]	11.40[b]	155.35[a]	303.40[b]	5.88[a]	11.75[b]	1.47[a]	1.53[b]

[a]Results are integrated to an s value of 2.06; end of probe forebody is at $s = 2.84$. [b]Results are integrated to an s value of 2.86; end of probe forebody is at $s = 2.84$.

Table 2 Effect of the variation in turbulent Lewis number on surface-heating and mass-loss rates for the 335-kg probe at a time of 49.13 s[a]

Le_T	$-\int_0^s \bar{q}_w^c \mathrm{d}\bar{A}$, MW		$\int_0^s \bar{q}_w^R \mathrm{d}\bar{A}$, MW		$\int_0^s (\bar{\rho}\bar{v})_w \mathrm{d}\bar{A}$, kg/s		Mass-loss ratio	
1.0	9.00[b]	15.00[c]	115.00[b]	212.00[c]	4.00[b]	7.70[c]	1.00[b]	1.00[c]
1.2	8.00[b]	13.90[c]	121.50[b]	222.80[c]	4.40[b]	8.00[c]	1.10[b]	1.04[c]
0.8	7.90[b]	14.11[c]	112.00[b]	206.50[c]	3.85[b]	7.50[c]	0.96[b]	0.97[c]

[a]Employs standard two-layer eddy-viscosity model of Cebeci. [b]Results are integrated to an s value of 2.06. [c]Results are integrated to an s value of 2.86, end of probe forebody is at $s = 2.84$.

these physical events in absence of any measurements may be more appropriate for the Galileo probe design.

Acknowledgments

The useful suggestions made by D.M. Bushnell and R.D. Watson of NASA Langley are gratefully acknowledged.

References

[1]Moss, J.N. and Simmonds, A.L., "Galileo Probe Forebody Flowfield Predictions During Jupiter Entry," AIAA Paper 82-0874, 1982.

[2]Cebeci, T., "Behavior of Turbulent Flow Near a Porous Wall with Pressure Gradient," *AIAA Journal,* Vol. 8, Dec. 1970, pp. 2152-2156.

[3]Anderson, E.C. and Moss, J.N., "Numerical Solution of the Hypersonic Viscous-Shock-Layer Equations for a Laminar, Transitional, and Turbulent Flow of a Perfect Gas Over Blunt Axially Symmetric Bodies," NASA TN D-7865, 1975.

[4]Gupta, R.N., "Turbulence Modeling of Flowfields With Massive Surface Ablation," AIAA Paper 82-0198, 1982.

[5]Varner, M.O. and Adams, J.C. Jr., "Variable Edge Entropy and Low Reynolds Number Effects on Hypersonic Turbulent Boundary Layers," AIAA Paper 80-0131, 1980.

[6]Johnson, C.B. and Bushnell, D.M., "Power-Law Velocity-Profile-Exponent Variations With Reynolds Number, Wall Cooling, and Mach Number in a Turbulent Boundary Layer," NASA TN D-5753, 1970.

[7]Bushnell, D.M., Cary, A.M., Jr. and Harris, J.E., "Calculation Methods for Compressible Turbulent Boundary Layers—1976," NASA SP-422, 1977.

[8]Keyes, J.W., "Correlation of Turbulent-Shear Layer Attachment Peak Heating Near Mach 6," *AIAA Journal,* Vol. 15, Dec. 1977, pp. 1821-1823.

Procedure for Generating Ground Wind Environments for Shuttle Liftoff Studies

George H. Fichtl* and Clark Brown†
NASA Marshall Space Flight Center, Huntsville, Alabama

Background

THIS Note provides a procedure for generating ground wind environments for Monte Carlo Shuttle liftoff and related studies. The procedure is based on a random selection of peak wind speeds at the 18.3 m level from which the mean wind profile and turbulence intensities are derived.[1] Random selection of mean wind direction is also used. The simulation of longitudinal and lateral turbulence components are obtained from a turbulence simulation tape as described in Refs.

Received Dec. 10, 1982; revision received Feb. 9, 1983.

*Chief, Fluid Dynamics Branch, Atmospheric Sciences Division. Associate Fellow AIAA.

†Aerospace Engineer, Environmental Applications Branch, Atmospheric Sciences Division.